Proceedings of the Seventh International Conference on
Railway Technology: Research, Development and Maintenance
Edited by: J. Pombo
Civil-Comp Conferences, Volume 15, Paper 18.5
Civil-Comp Press, Edinburgh, United Kingdom, 2026
ISSN: 2753-3239, doi: 10.4203/ccc.15.18.5


# Simplified Constraint-Based Wheel-Rail Contact Modelling

**E. M. Snellman[1], K. Koskinen[2] and X. Yu[1]**

**[1] Machine Dynamics Group, Faculty of Engineering and Natural Sciences, Tampere University, Finland**
**[2] Mechatronics Research Group, Faculty of Engineering and Natural Sciences, Tampere University, Finland**

## Abstract

In real-time simulations of railway vehicles, accurate but computationally efficient methods to solve wheel-rail contact problems are needed. In this work, three constraint-based contact methods are compared for modelling wheel–rail of interaction within the framework of railway multibody dynamics. The first method employs a lookup-table approach, in which wheel–rail contact information is interpolated from precomputed tables during the dynamic simulation. The second method uses analytical exponential functions to represent the wheel–rail contact geometry, allowing the contact information to be evaluated analytically during the simulation. The third method simplifies the contact geometry by using constant parameters, such as equivalent conicity, throughout the dynamic simulation. These approaches are implemented on a dynamic model of a wheelset on a tangent track with irregularities, and the results are compared against commercial software Simpack. Both new and worn wheel profiles are considered. The results show that the approaches based on lookup tables and analytical exponential functions are able to model the variations on vertical-lateral wheel-rail contact forces, while constant parameter approach underestimates this.

**Keywords:** multibody dynamics, contact force, lookup table, exponential fitting, worn wheels, friction.

# 1 Introduction

Wheel-rail interaction has a major influence in the dynamics of railway vehicles. Accurate modelling of wheel-rail contact is essential for prediction of contact forces, which are further needed for assessment of derailment safety criteria and prediction of wheel-rail wear. Due to complex shapes of the interacting geometries and frictional effects, the wheel-rail contact problem is highly non-linear. Wheel–rail contact modelling approaches for normal contact forces range from elastic-based methods, such as Hertzian and non-Hertzian theories [1], to constraint-based methods, including lookup-table and knife-edge contact approaches [2]. For tangential contact forces, modelling approaches vary from the linear Kalker theory to nonlinear formulations, such as the Polach model [1]. Naturally, the very accurate models are often computationally expensive, limiting their use in real-time simulations, needed in state observation and control applications for instance.

In addition to modelling of the contact behaviour, finding the contact locations for each time step poses an another challenge in multibody simulations of railway vehicles. The contact search can be done with online approaches, where the contact points are solved for each time step separately, or with offline approaches, where the contact points are calculated in preprocessing stage for range of wheelset relative position to tracks [2]. In the offline approach, lookup tables (LUT) of the preprocessed results are used to interpolate contact location for given wheelset displacement during simulation [3]. Contact lookup tables provide a computationally efficient way to determine the contact location.

This work compares three constraint-based approaches to model wheel-rail contact in dynamic simulation of railway vehicles. The approaches are compared using a single wheelset running on a straight track with irregularities. The first approach utilizes lookup tables of rolling radius, contact angle, and wheel and rail curvatures for given lateral displacement of the wheelset and gauge irregularity. The results are used to calculate contact patch semi-axes according to Hertzian theory, which are further used in tangential contact force calculation according to Polach contact model [4]. The second approach utilizes exponential curve fitting instead of lookup tables in definition of contact point information and simplified calculation of contact patch semi-axes. The third approach assumes constant conicity of the wheels. The results of the three approaches are compared to results obtained with commercial software Simpack.

# 2 Methods

In this section, the dynamic model of a single unsuspended wheelset is described. The wheelset equations of motion consider three degrees of freedom, which are the lateral displacement $y_{ws}$, yaw angle $\psi_{ws}$ , and pitch angle $\theta_{ws}$ of the wheelset. The lateral displacement and rotations of the wheelset are with respect to track frame, defined by $X_t$, $Y_t$ and $Z_t$ -axes. The wheelset kinematics is illustrated in Figure 1. The vector of generalized coordinates for the single wheelset can be written as:

$$\mathbf{q} = \begin{bmatrix} y_{ws} & \psi_{ws} & \theta_{ws} \end{bmatrix}^T. \tag{1}$$

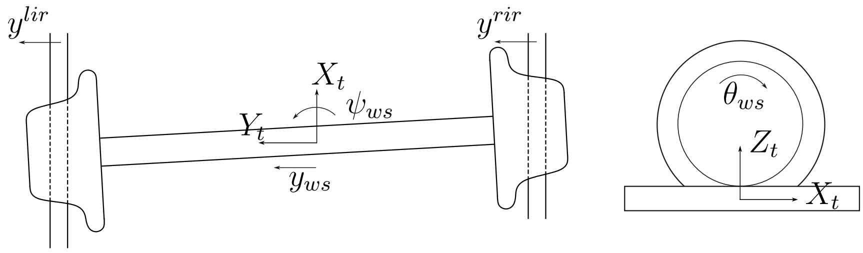


Figure 1: Wheelset model kinematics

The wheelset dynamics is studied on irregular track. In this work, only lateral and gauge irregularities are considered. These irregularities are defined by equations:

$$al = (y^{lir} + y^{rir})/2 \tag{2}$$

$$ga = y^{lir} - y^{rir}, \tag{3}$$

where $al$ is alignment irregularity, $ga$ is gauge irregularity, and $y^{lir}$ and $y^{rir}$ are the lateral displacements of left and right rail profiles from their ideal positions measured along $Y_t$-axis.

## 2.1 Contact geometry modelling approaches

In this study, wheelset with new S1002 wheel profile and a worn S1002 profile is paired with new UIC60 rail profile. The new and worn wheel profiles are illustrated in Figure 2. From Figure 2 can be seen that the worn profile has wear in both tread and flange sections, both measurable in millimetre range.

For the wheelset, three approaches to find the contact location and to model the contact geometry are used. The first approach uses contact lookup tables with wheelset lateral displacement with respect to track centerline and gauge irregularity as its entries. The lateral position of the wheelset with respect to the track centerline $y'_{ws}$ can be defined with equation:

$$y'_{ws} = y_{ws} - al. \tag{4}$$

The contact lookup tables are formed by assuming the wheelset yaw angle as zero, and by searching the contact location for a range of values for $y'_{ws}$ and $ga$. The contact point search is done with algorithm presented in [5]. From the contact search results, the rolling radius, contact angle, and the wheel and rail curvatures are obtained, which are then used to form lookup tables of these results. In Figure 3, the left wheel rolling

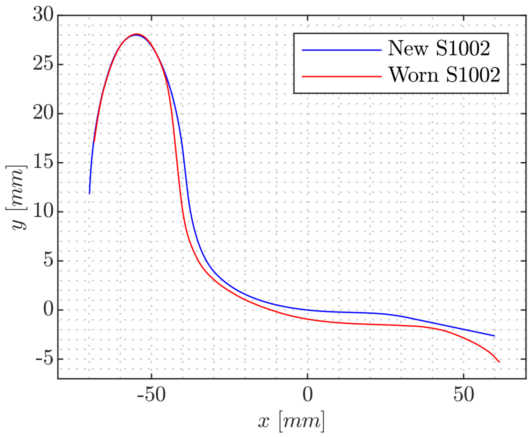


Figure 2: New and worn S1002 wheel profiles

radius and contact angle used for lookup table generation are compared to plots obtained from Simpack for nominal gauge of 1.435 m and rail inclination of 1/40. From Figure 3 can be seen that the rolling radius and contact angle of LUT method match well with Simpack equivalents.

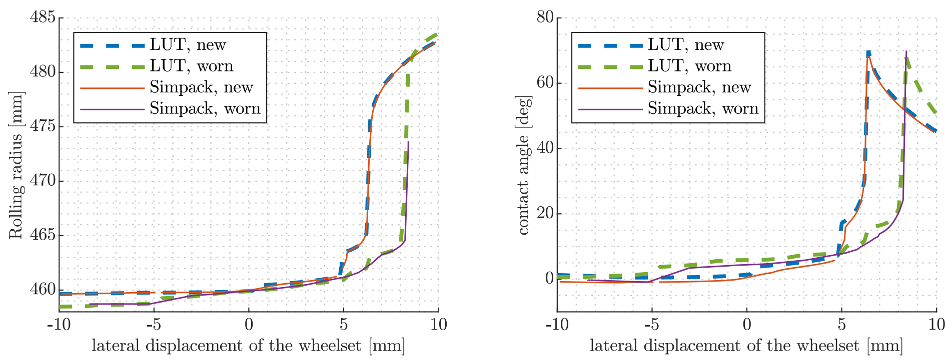


Figure 3: Rolling radius and contact angle for new and worn wheels

In the second contact modelling approach, the lookup tables of rolling radius and contact angle are replaced by fitting exponential functions to the rolling radius and contact angle data as in [6]. The functions for rolling radius and contact angle are defined by equations:

$$r(y'_{ws}, ga) = r_1 + r_2 e^{r_3(y'_{ws} - ga/2)} \tag{5}$$

$$\delta(y'_{ws}, ga) = \delta_1 e^{\delta_2(y'_{ws} - ga/2)} + \delta_3 e^{\delta_4(y'_{ws} - ga/2)} \tag{6}$$

where $r$ is the rolling radius, $\delta$ is the contact angle, and $r_{1,2,3}$ and $\delta_{1,2,3}$ are parameters of the rolling radius and contact angle functions obtained through curve fitting. The curves are fitted to rolling radius and contact angle data obtained from contact search for zero gauge irregularity, thus $ga$ is set to zero in Equations (5-6) during fitting process. The curve fitting is performed with Matlab *lsqcurvefit* function. In Figure 4, the fitted rolling radius and contact angle functions are presented for the new and worn wheels. The fitting is done by prioritizing good fit at the tread region, and in Figure 4 can be seen that rather good fit is obtained for both rolling radius and contact angle before point of flange contact, which is at 6 mm lateral displacement for new wheel profile and at 8 mm lateral displacement for worn wheel profile. After the point of flange contact, both fitting functions underestimate rolling radius and contact angle notably.

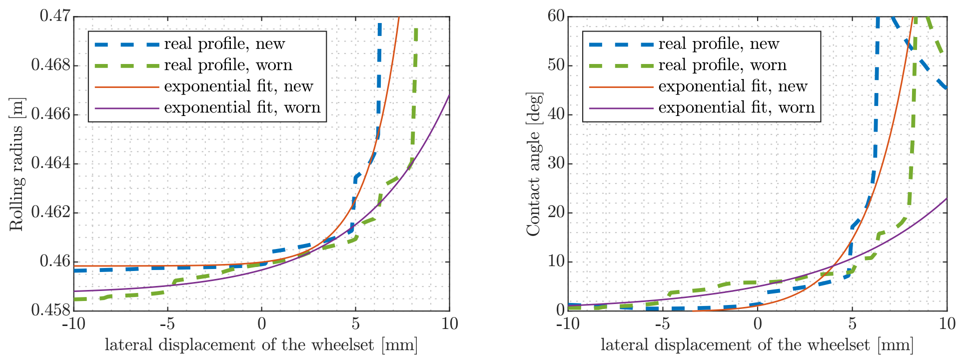


Figure 4: Rolling radius and contact angle functions fitted to data

In the third contact modelling approach pure conical wheels are assumed. For the pure conical wheels the contact angle is constant, and the rolling radiuses of left and right wheels vary linearly with wheelset lateral displacement, defined by equivalent conicity. The equivalent conicity values are obtained from Simpack for 3 mm amplitude, which is 0.178 for new wheels and 0.174 for worn wheels. For contact angles the value at 3 mm displacement is used for both left and right right wheels, which is 0.0920 rad for new wheels and 0.1282 rad for worn wheels.

## 2.2 Simplified contact ellipse calculation

For the calculation of tangential forces Polach contact model [4] is used, which assumes elliptical contact area according to Hertz theory. The contact ellipse semi-axes $a$ and $b$ can be calculated with equations:

$$a = m\,(3\pi F_n(K_1 + K_2)/4K_3)^{1/3} \tag{7}$$
$$b = n\,(3\pi F_n(K_1 + K_2)/4K_3)^{1/3} \tag{8}$$

where $m$, $n$ and $K_3$ are parameters dependent on curvatures of contacting bodies in contact point, $F_n$ is normal contact force, $K_1$ and $K_2$ are parameters dependent on material properties of bodies in contact [7]. In these equations $m$, $n$ and $K_3$ are not constants due to changes in curvatures for different contact points. For the exponential fit and linear conicity contact models the curvatures are assumed to be constant, which makes contact ellipse semi-axes only dependent on normal force. With this simplification the ratio of contact ellipse semi-axes remains constant, yielding constant Kalker's coefficients [7]. With these simplifications, the use of lookup tables in the determination of wheel-rail contact forces is avoided.

## 2.3 Calculation of normal contact forces

In this work, the calculation of normal contact forces is based on the vertical and moment balance of the wheelset. In the calculation of the force and moment balance, the yaw angle of wheelset is assumed as zero. The free body diagram of the wheelset is presented in Figure 5, where the forces acting on the wheelset in $Y_tZ_t$-plane are illustrated. In this figure, $\bar{\mathbf{F}}_{cyL}$ and $\bar{\mathbf{F}}_{cyR}$ are lateral friction force vectors of left and right wheels, $\bar{\mathbf{F}}_g$ is the gravitational force vector, $\bar{\mathbf{N}}_L$ and $\bar{\mathbf{N}}_R$ are normal contact force vectors of left and right wheels, and $\bar{\mathbf{u}}_{C_{lw}}$ and $\bar{\mathbf{u}}_{C_{rw}}$ are position vectors from wheelset centre of mass to the left and right contact points. All vectors are expressed in the track frame. The superelevation angle $\varphi_{se}$ in this work is zero.

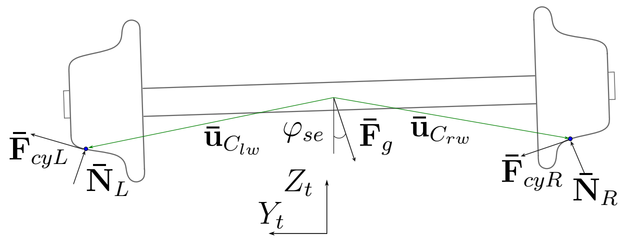


Figure 5: Wheelset forces in $Y_tZ_t$-plane

The normal contact forces can be calculated from balance of forces acting along $Z_t$-axis and moments acting over $X_t$-axis. These balance equations can be expressed as:

$$\begin{bmatrix} (\bar{\mathbf{n}}_{lc})_z & (\bar{\mathbf{n}}_{rc})_z \\ \bar{\mathbf{u}}_{C_{lw}} \times \bar{\mathbf{n}}_{lc} & \bar{\mathbf{u}}_{C_{rw}} \times \bar{\mathbf{n}}_{rc} \end{bmatrix} \begin{bmatrix} f_L^n \\ f_R^n \end{bmatrix} = \begin{bmatrix} -(\bar{\mathbf{F}}_{cyL})_z - (\bar{\mathbf{F}}_{cyR})_z - (\bar{\mathbf{F}}_g)_z \\ -\bar{\mathbf{u}}_{C_{lw}} \times \bar{\mathbf{F}}_{cyL} - \bar{\mathbf{u}}_{C_{rw}} \times \bar{\mathbf{F}}_{cyR} \end{bmatrix} \tag{9}$$

where $\bar{\mathbf{n}}_{lc}$ and $\bar{\mathbf{n}}_{rc}$ are unit vectors in direction of $\bar{\mathbf{N}}_L$ and $\bar{\mathbf{N}}_R$, and $f_L^n$ and $f_R^n$ are the normal force amplitudes of normal forces of $N_L$ and $N_R$ respectively. In Equation (9) subscript $z$ refers to taking component of the vector along $Z_t$-axis. The calculation of normal forces with Equation (9) requires the friction forces to be known, while the calculation of friction forces requires the normal forces to be known. To avoid iterative solution of both forces, the friction forces of previous time step are used in the calculation of normal forces of current time step.

## 2.4 Results

The three contact modelling approaches are compared on straight track with only alignment and gauge irregularities present. The track irregularities are presented in Figure 6. The simulations are carried out with 5 m/s initial velocity and with 0.4 coefficient of friction of wheel rail interface, representing dry conditions [8]. The simulated lateral displacement and yaw angle results with new and worn wheel profiles are presented in Figure 7. From the results can be seen that with new profiles the lateral displacement and yaw angle of all three models follow Simpack results rather well up to roughly 40 m, after which all three models start to have more deviation with respect to Simpack results. With worn profiles lateral displacement and yaw angle responses of the three models follow Simpack with better accuracy than in case of new wheels, but the lookup table and exponential fit models start to diverge more clearly around 80 m.

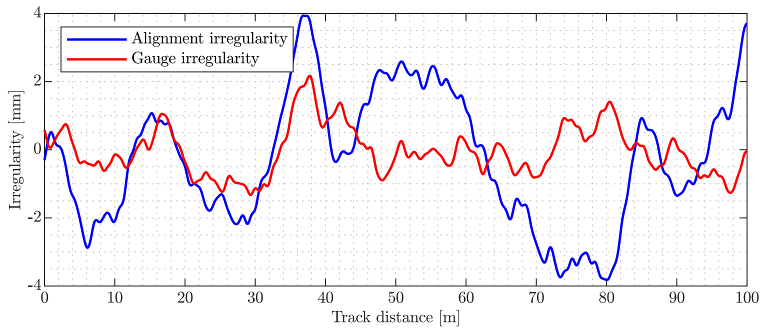


Figure 6: Track alignment and lateral irregularities

The contact forces obtained with new wheels are presented in Figure 8 for the left wheel, showing clear differences between the approaches. The lookup table model captures the Simpack lateral friction forces with the best accuracy. The exponential fit model is able to capture the range of the lateral friction force up to 40 meters, while constant conicity model shows only very small variation of lateral force. After 40 meters the exponential fit model begins to overestimate the lateral force variation, when the lateral displacement and yaw angle also start to diverge from Simpack results. The normal force plot from Simpack presents many peaks that none of the three approaches capture well, but the overall level is captured with all models. All three models also predict some low frequency variation of normal contact force, but none of the approaches capture the high frequency variation present in Simpack results.

The contact forces obtained with worn wheels are presented in Figure 9 for the left wheel. Again the lookup table approach captures the lateral friction forces with the best accuracy, but it diverges from Simpack results from 80 m onwards. The exponential fit model again predicts the variation in lateral forces better than the constant conicity model, but it also diverges from 80 m onwards. The normal force plot of Simpack contains much fewer peaks than with new profiles, but it still contains high

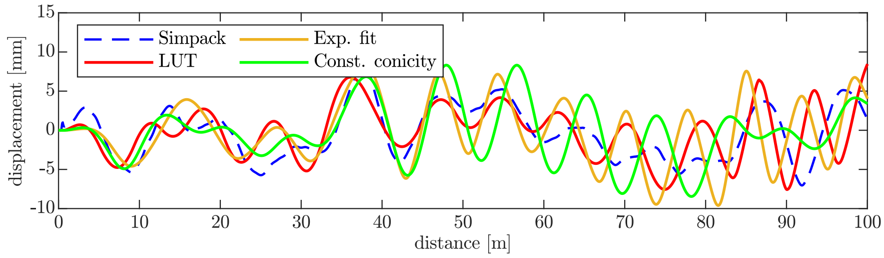


(a) lateral displacement, new profile

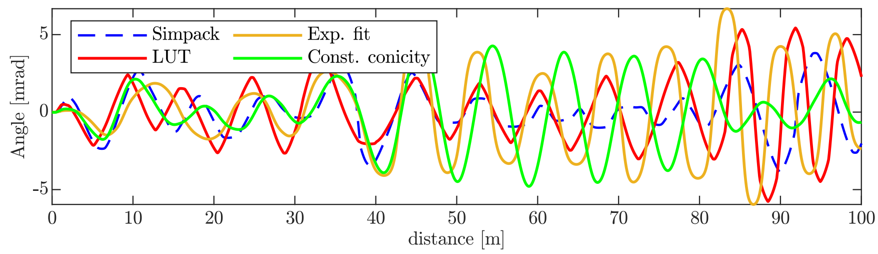


(b) yaw angle, new profile

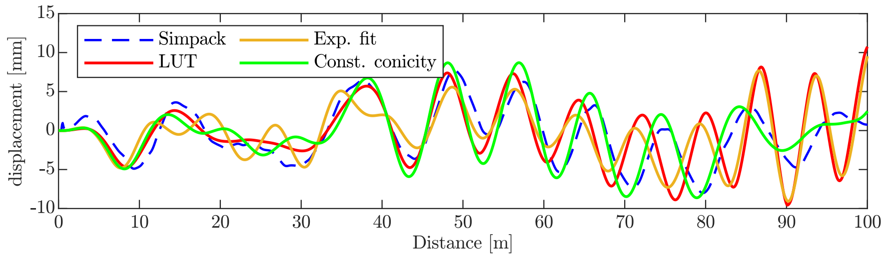


(c) lateral displacement, worn profile

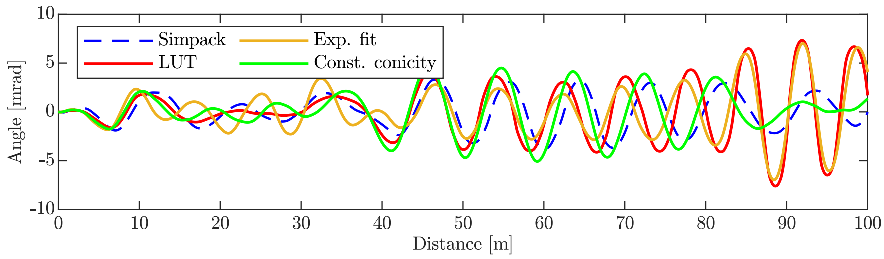


(d) yaw angle, worn profile

Figure 7: Simulated lateral displacement and yaw angle results

frequency variation that the three approaches are not able to model.

# 3 Conclusions

In this paper, three constraint-based contact methods for modelling wheel–rail interaction are compared. The methods model the contact geometry by using either contact lookup tables, analytical exponential functions, or constant parameters. The

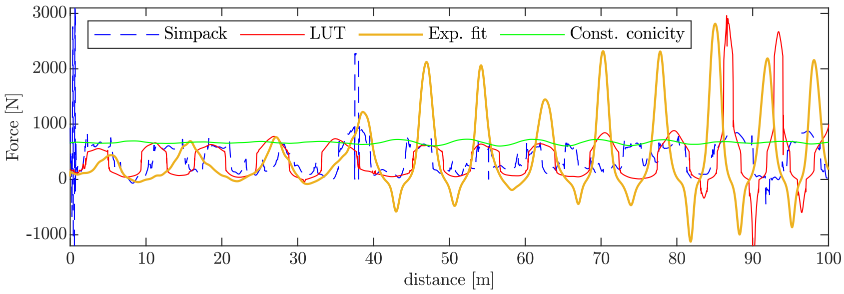


(a) Lateral friction force

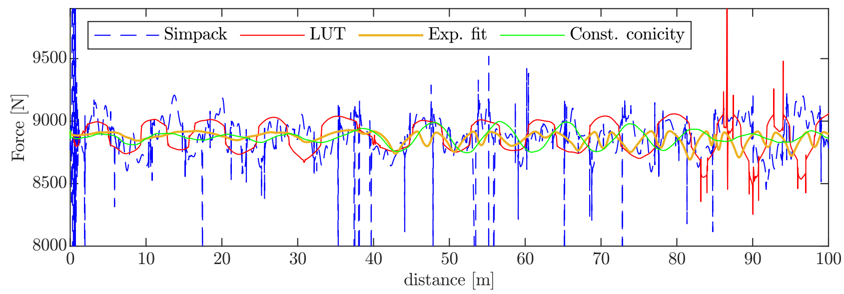


(b) Normal force

Figure 8: Simulated contact forces results for left wheel with new wheel profile

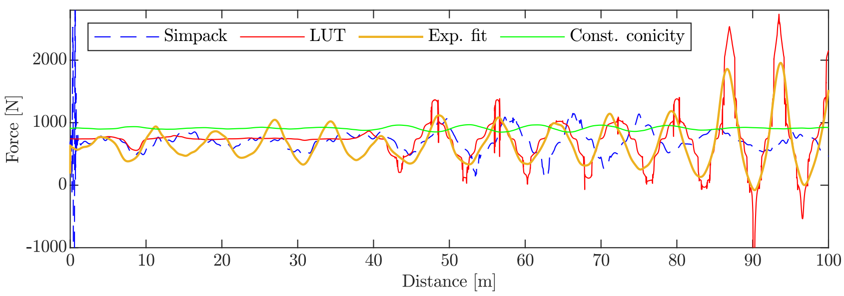


(a) Lateral friction force

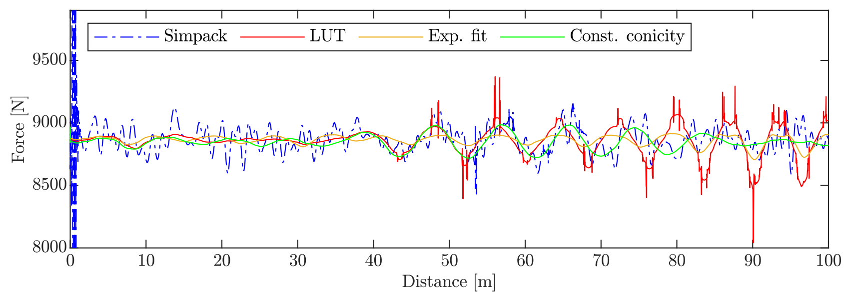


(b) Normal force

Figure 9: Simulated contact forces results for left wheel with worn wheel profile

approaches are studied with a dynamic model of single wheelset running on straight track, and the models are compared against commercial software Simpack.

The results show that all approaches can predict the lateral displacement and yaw angle oscillations of wheelset with reasonable accuracy, but all results deviate from Simpack results in the studied time window. The lateral contact friction force variation is captured with the highest accuracy by lookup table approach, but the exponential fit approach is also capable of capturing the variations in lateral friction force. The approach using pure constant conicity predicts very low variation of lateral contact friction force. With new wheel profiles, Simpack results show many peaks in normal contact force graphs, that none of the three approaches are able to predict accurately. Only lookup table approach produces force peaks in the normal contact force results. Otherwise, all three approaches can predict low frequency variation in normal contact force.

The three simplified contact modelling approaches presented here provide computationally lightweight options to model wheel-rail contacts to applications where computational efficiency is demanded. In future work, the contact modelling approaches will be compared in simulations including other vehicle components, such as bogies and car bodies, and in more complex running scenarios.

# References


[1] S.Z. Meymand, A. Keylin, M. Ahmadian, ”A survey of wheel–rail contact models for rail vehicles”, Vehicle System Dynamics, 54(3), 386-428, 2016. doi: 10.1080/00423114.2015.1137956.

[2] J. L. Escalona, X. Yu, J. F Aceituno, ”Wheel–rail contact simulation with lookup tables and KEC profiles: a comparative study”, Multibody System Dynamics, 52(4), 339-375, 2021.

[3] X. Yu, J. F. Aceituno, E. Kurvinen, M. K. Matikainen, P. Korkealaakso, A. Rouvinen, D. Jiang, J. L. Escalona, A. Mikkola, “Comparison of numerical and computational aspects between two constraint-based contact methods in the description of wheel/rail contacts,” Multibody System Dynamics, 54(3), 303-344, 2022.

[4] O. Polach, ”A fast wheel-rail forces calculation computer code”, Vehicle System Dynamics, 33, 728–739, 1999.

[5] Z. Li, ”Wheel-rail rolling contact and its application to wear simulation”, PhD thesis, Delft University of Technology, Delft, The Netherlands, 2002.

[6] A. Keck, C. Schwarz, T. Meurer, A. Heckmann, G. Grether,”Estimating the wheel lateral position of a mechatronic railway running gear with nonlinear wheel–rail geometry”, Mechatronics, 73, 102457, 2021. doi: 10.1016/j.mechatronics.2020.102457

[7] A.A. Shabana, K.E. Zaazaa, H. Sugiyama, ”Railroad vehicle dynamics: a computational approach”, CRC press, Boca Raton, United States, 2007.

[8] O. Polach, ”Creep forces in simulations of traction vehicles running on adhesion limit”, Wear, 258(7-8), 992-1000, 2005. doi: 10.1016/j.wear.2004.03.046